Wireless *Non-Radiative* Energy Transfer

Aristeidis Karalis, J.D.Joannopoulos, and Marin Soljačić

Center for Materials Science and Engineering and Research Laboratory of Electronics, MIT, 77 Massachusetts Avenue, Cambridge, MA 02139

We investigate whether, and to what extent, the physical phenomenon of long-lifetime resonant electromagnetic states with localized slowly-evanescent field patterns can be used to transfer energy efficiently, even in the presence of extraneous environmental objects. Via detailed theoretical and numerical analyses of typical real-world model-situations and realistic material parameters, we establish that such a non-radiative scheme could indeed be practical for medium-range wireless energy transfer.

I. Introduction

In the early days of electromagnetism, before the electrical-wire grid was deployed, serious interest and effort was devoted (most notably by Nikola Tesla [1]) towards the development of schemes to transport energy over long distances without any carrier medium (e.g. wirelessly). These efforts appear to have met with little, if any, success. Radiative modes of omni-directional antennas (which work very well for information transfer) are not suitable for such energy transfer, because a vast majority of energy is wasted into free space. Directed radiation modes, using lasers or highly-directional antennas, can be efficiently used for energy transfer, even for long distances (transfer distance $L_{TRANS} \gg L_{DEV}$, where L_{DEV} is the characteristic size of the device), but require existence of an uninterruptible line-of-sight and a complicated tracking system in the case of mobile objects. Rapid development of autonomous electronics of recent years (e.g. laptops, cell-phones, house-hold robots, that all typically rely on chemical energy storage) justifies revisiting investigation of this issue. Today, we face a different challenge than Tesla: since the existing electrical-wire grid carries energy *almost* everywhere, even a medium-range wireless energy transfer would be quite useful. One scheme currently used

for some important applications relies on induction, but it is restricted to very close-range ($L_{TRANS} \ll L_{DEV}$) energy transfers [2,3,4,5]. In contrast to the currently existing schemes, we investigate the feasibility of using long-lived oscillatory resonant electromagnetic modes, with localized slowly evanescent field patterns, for wireless *non-radiative* energy transfer. The basis of this method is that two same-frequency resonant objects tend to couple, while interacting weakly with other off-resonant environmental objects. The purpose of the present paper is to quantify this mechanism using specific examples, namely quantitatively address the following questions: up to which distances can such a scheme be efficient and how sensitive is it to external perturbations? Our detailed theoretical and numerical analysis show that a mid-range ($L_{TRANS} \approx few * L_{DEV}$) wireless energy-exchange can actually be achieved, while suffering only modest transfer and dissipation of energy into other off-resonant objects. The omnidirectional but stationary (non-lossy) nature of the near field makes this mechanism suitable for mobile wireless receivers. It could therefore have a variety of possible applications including for example, placing a source (connected to the wired electricity network) on the ceiling of a factory room, while devices (robots, vehicles, computers, or similar) are roaming freely within the room. Other possible applications include electric-engine buses, RFIDs, and perhaps even nano-robots.

II. Range and rate of coupling

The range and rate of the proposed wireless energy-transfer scheme are the first subjects of examination, without considering yet energy drainage from the system for use into work. An appropriate analytical framework for modeling this resonant energy-exchange is that of "coupled-mode theory" [6]. In this picture, the field of the system of two resonant objects 1 and 2 is approximated by $\mathbf{F}(\mathbf{r},t) \approx a_1(t)\mathbf{F}_1(\mathbf{r}) + a_2(t)\mathbf{F}_2(\mathbf{r})$, where $\mathbf{F}_{1,2}(\mathbf{r})$ are the eigenmodes of 1 and 2 alone, and then the field amplitudes $a_1(t)$ and $a_2(t)$ can be shown [6] to satisfy, to lowest order:

$$\begin{aligned} \frac{da_1}{dt} &= -i\left(\omega_1 - i\Gamma_1\right)a_1 + i\kappa a_2 \\ \frac{da_2}{dt} &= -i\left(\omega_2 - i\Gamma_2\right)a_2 + i\kappa a_1 \end{aligned}, \qquad (1)$$

where $\omega_{1,2}$ are the individual eigenfrequencies, $\Gamma_{1,2}$ are the resonance widths due to the objects' intrinsic (absorption, radiation etc.) losses, and κ is the coupling coefficient. Eqs.(1) show that at exact resonance ($\omega_1=\omega_2$ and $\Gamma_1=\Gamma_2$), the eigenmodes of the combined system are split by 2κ; the energy exchange between the two objects takes place in time π/κ and is nearly perfect, apart for losses, which are minimal when the coupling rate is much faster than all loss rates ($\kappa \gg \Gamma_{1,2}$).[†] It is exactly this ratio $\kappa/\sqrt{\Gamma_1\Gamma_2}$ that we will set as our figure-of-merit for any system under consideration for wireless energy-transfer, along with the distance over which this ratio can be achieved.[‡]

Therefore, our non-radiative-coupling application requires resonant modes of high $Q=\omega/2\Gamma$ for low (slow) intrinsic-loss rates Γ and with evanescent tails significantly longer than the characteristic sizes of the objects for strong (fast) near-field-coupling rate κ over large distances. This is a regime of operation that has *not* been studied extensively, since one usually prefers short tails to minimize interference with nearby devices. Unfortunately, the radiation Q usually decreases along with the resonator size, so the above characteristics can only be achieved using resonant objects of finite subwavelength size for large relative extent of the non-radiative near field (set typically by the wavelength and quantified rigorously by the "radiation caustic") into the surrounding air. Such subwavelength resonances are often accompanied with a high radiation Q, so this will typically be the appropriate choice for the possibly-mobile resonant device-object d. Note, though, that the resonant source-object s will in practice often be immobile and with less stringent restrictions on its allowed geometry and size, which can be therefore chosen large enough so that its radiative losses are negligible (using for example waveguides with guided modes tuned close to the "light line" in air for slow exponential decay therein).

The proposed scheme is very general and *any* type of resonant structure (e.g. electromagnetic, acoustic, nuclear) satisfying the above requirements can be used for its

[†] The limits of validity of the coupled-mode-theory model include this optimal regime of operation, since the weak-coupling condition $\kappa \ll \omega_{1,2}$ also holds for medium-distance coupling, and thus the use of this model is justified and the parameters κ, $\Gamma_{1,2}$ are well defined.

[‡] Note that interference effects (not captured by coupled-mode theory) between the radiation fields of the two initial single-object modes result in radiation-Γ's for the eigenmodes of the system that are different than but approximately average to the initial single-object radiation-Γ's.

implementation. As examples and for definiteness, we choose to work with two well-known, but quite different, electromagnetic resonant systems: dielectric disks and capacitively-loaded conducting-wire loops. Even without optimization, and despite their simplicity, both will be shown to exhibit acceptably good performance.

a) Dielectric disks

Consider a 2D dielectric disk resonant object of radius *r* and permittivity ε surrounded by air that supports high-*Q* whispering-gallery modes (Figure 1). All subsequent calculations for this type of resonant disks were performed using numerical finite-difference frequency-domain (FDFD) mode-solver simulations (with a resolution of *30pts/r*), but analytical methods were also used, when applicable, to verify the results.

The loss mechanisms for the energy stored inside such a resonant system are radiation into free space and absorption inside the potentially lossy disk material. High-radiation-*Q* and long-tailed subwavelength resonances can be achieved, when the dielectric permittivity ε is as large as practically possible and the azimuthal field variations (of principal number *m*) are slow (namely *m* is small). Two such TE-polarized dielectric-disk modes with the favorable characteristics $Q^{rad} = 1992,\ \lambda / r = 20$ and $Q^{rad} = 9100,\ \lambda / r = 10$ are presented in Figure 1, and imply that for a properly designed resonant dielectric object a value of $Q^{rad} \geq 2000$ should be achievable. Material absorption is related to the loss tangent, $Q^{abs} \sim \varepsilon / \mathrm{Im}\{\varepsilon\}$, and we will assume $Q^{abs} \geq 10^4$.

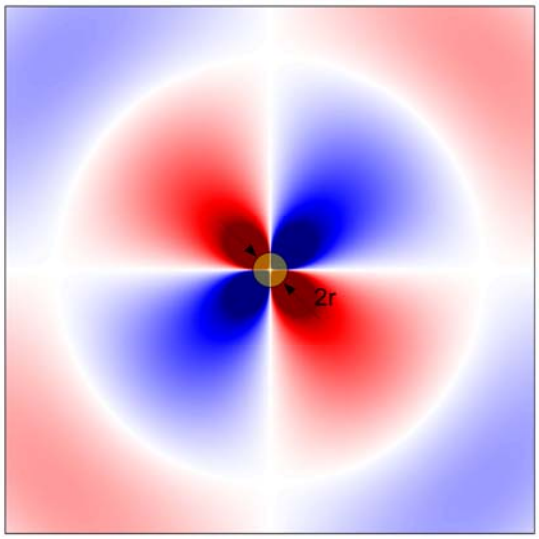

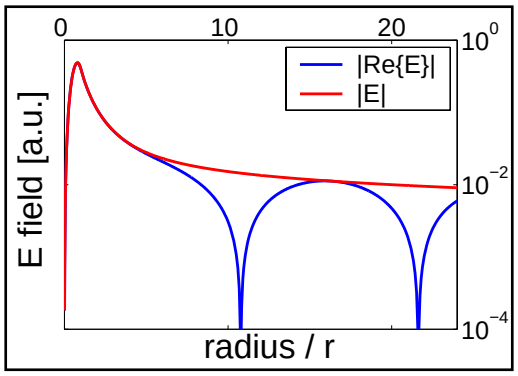

single disk	λ/r	Q^{rad}	Q^{abs}	$Q=\omega/2\Gamma$
Re{ε}=147.7, m=2	**20**	**1992**	**10093**	**1664**
Re{ε}=65.6, m=3	10	9100	10094	4786

Figure 1: Numerical FDFD results for a 2D high-ε disk of radius r along with the electric field (pointing out of the page) of its resonant whispering-gallery mode.[§] [Side plot: shape of the modal field. In air, it follows a Hankel-function form: note the initial exponential-like regime (with long tails compared to the small disk size), followed by the oscillatory/radiation regime (whose presence means that energy is slowly leaking out of the disk).] For the tabulated results material loss Im{ε}/Re{ε}=10^{-4} has been used. *{The specific parameters of the shown plot are highlighted with bold in the Table.}*

Note that the required values of ε, shown in Figure 1, might at first seem unrealistically large. However, not only are there in the microwave regime (appropriate for meter-range coupling applications) many materials that have both reasonably high enough dielectric constants and low losses (e.g. Titania: $\varepsilon \approx 96$, $Im\{\varepsilon\}/\varepsilon \approx 10^{-3}$; Barium tetratitanate: $\varepsilon \approx 37$, $Im\{\varepsilon\}/\varepsilon \approx 10^{-4}$; Lithium tantalite: $\varepsilon \approx 40$, $Im\{\varepsilon\}/\varepsilon \approx 10^{-4}$; etc.) [7,8], but also ε could signify instead the effective index of other known subwavelength ($\lambda/r \gg 1$) surface-wave systems, such as surface-plasmon modes on surfaces of metal-like (negative-ε) materials [9] or metallo-dielectric photonic crystals [10].

To calculate now the achievable rate of energy transfer, we place two same disks at distance D between their centers (Figure 2). The FDFD mode-solver simulations give κ through the frequency splitting of the normal modes of the combined system, which are even and odd

[§] Note that for the 3D case the computational complexity would be immensely increased, while the physics should not be significantly different. For example, a spherical object of $\varepsilon=147.7$ has a whispering gallery mode with $m=2$, $Q^{rad}=13962$, and $\lambda/r=17$.

superpositions of the initial modes. Then for distances $D/r = 10-3$, and for non-radiative coupling such that $D \le r_C$, where r_C is the radius of the radiation caustic, we find (Figure 2) coupling-to-loss ratios in the range $\kappa/\Gamma \sim 1-50$. Although the achieved values do not fall in the ideal operating regime $\kappa/\Gamma \gg 1$, they are still large enough to be useful for applications, as we will see later on.

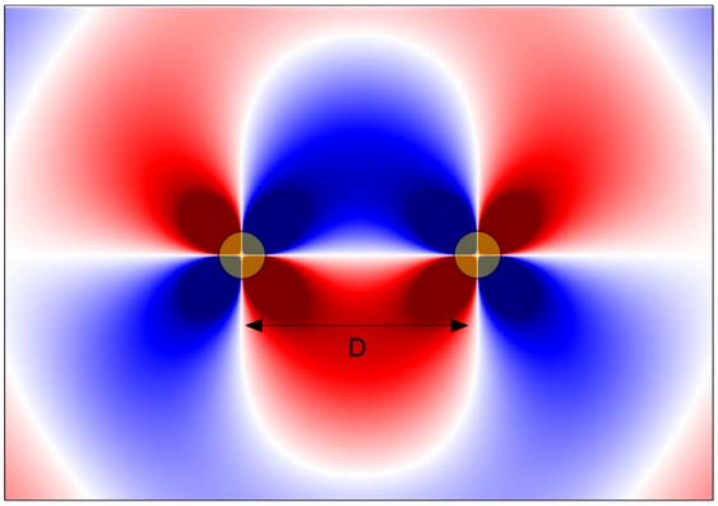

two disks	D/r	$\omega/2\kappa$	Q^{rad}	$Q=\omega/2\Gamma$	κ/Γ
Re{ε}=147.7, m=2	3	47	2478	1989	42.4
$\lambda/r \approx 20$	5	298	2411	1946	6.5
$Q^{abs} \approx 10096$	7	770	2196	1804	2.3
	10	**1714**	**2017**	**1681**	**1.0**
Re{ε}=65.6, m=3	3	144	7972	4455	30.9
$\lambda/r \approx 10$	5	2242	9240	4824	2.2
$Q^{abs} \approx 10096$	7	7485	9187	4810	0.6

Figure 2: Numerical FDFD results for medium-distance coupling between two resonant disks. If initially all the energy is in one disk, after some time ($t=\pi/2\kappa$) both disks are equally excited to one of the normal modes of their combined system. For the tabulated results the normal mode that is odd with respect to the line that connects the two disks is used, only distances for non-radiative ($D \le r_C$) coupling are considered, and the Γ's are taken to be the averages of the corresponding calculated Γ's of the two normal modes, where an increase/decrease in radiation Q for the system is due to destructive/constructive interference effects. *{The specific parameters of the shown plot are highlighted with bold in the Table.}*

b) Capacitively-loaded conducting-wire loops

Consider N loops of radius r of conducting wire with circular cross-section of radius a surrounded by air (Figure 3a). This wire has inductance $L = \mu_o N^2 r\left[\ln\left(8r/a\right)-2\right]$ [11], where μ_o is the magnetic permeability of free space, so connecting it to a capacitance C will make the loop resonant at frequency $\omega = 1/\sqrt{LC}$. The nature of the resonance lies in the periodic exchange of energy from the electric field inside the capacitor due to the voltage across it to the magnetic field in free space due to the current in the wire.

Losses in this resonant system consist of ohmic loss inside the wire and radiative loss into free space. In the desired subwavelength-loop ($r \ll \lambda$) limit, the resistances associated with the two loss channels are respectively $R_{abs} = \sqrt{\mu_o \rho \omega / 2} \cdot Nr/a$ and $R_{rad} = \pi/6 \cdot \eta_o N^2 \left(\omega r/c\right)^4$ [12], where ρ is the resistivity of the wire material and $\eta_o \approx 120\pi\ \Omega$ is the impedance of free space. The quality factor of such a resonance is then $Q = \omega L/\left(R_{abs}+R_{rad}\right)$ and is highest for some optimal frequency determined by the system parameters: at low frequencies it is dominated by ohmic loss and at high frequencies by radiation. The examples presented in Figure 3a show that at this optimal frequency expected quality factors in the microwave are $Q^{abs} \sim (1000-1500)\cdot N$ and $Q^{rad} \sim 7500-10000$ at $\lambda/r \sim 60-80$, namely suitable for near-field coupling.

The rate for energy transfer between two loops 1 and 2 at distance D between their centers (Figure 3b) is given by $\kappa_{12} = \omega M/2\sqrt{L_1 L_2}$, where M is the mutual inductance of the two loops. In the limit $r \ll D \ll \lambda$ one can use the quasi-static result $M = \pi/4 \cdot \mu_o N_1 N_2 \left(r_1 r_2\right)^2/D^3$, which means that $\omega/2\kappa \sim \left(D/\sqrt{r_1 r_2}\right)^3$. The examples presented in Figure 3b show that for medium distances $D/r = 10-3$ the expected coupling-to-loss ratios, which peak at a frequency between those where the single-loop $Q_{1,2}$ peak, are in the range $\kappa/\Gamma \sim 0.1-10$. Now, we are even further from the optimal regime $\kappa/\Gamma \gg 1$, but still these values will be shown to be viable.

It is important to appreciate the difference between this inductive scheme and the well-known close-range inductive schemes for energy transfer [2] in that those schemes are *non-resonant*. Using coupled-mode theory it is easy to show that, keeping the geometry and the energy stored at the source fixed, the presently proposed resonant-coupling inductive mechanism allows for $\sim Q^2$ ($\sim 10^6$) times more power delivered for work at the mid-range distant device than the traditional non-resonant mechanism, and this is why mid-range energy transfer is now possible. Capacitively-loaded conductive loops are actually being widely used as resonant antennas (for example in cell phones), but those operate in the far-field regime with $D/r \gg 1$, $r/\lambda \sim 1$, and the radiation Q's are intentionally designed to be small to make the antenna efficient, so they are not appropriate for energy transfer.

(a)

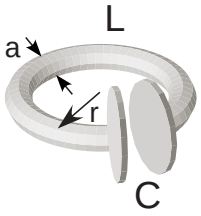

(b)

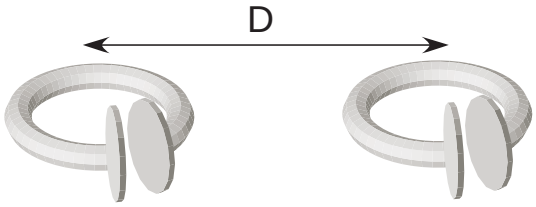

single loop	λ / r	Q^{rad}	Q^{abs}	$Q = \omega/2\Gamma$
r=1cm, a=1mm	79	9025	1419	1227
r=30cm, a=2mm	59	7977	1283	1105
r=1m, a=4mm	60	9315	1531	1315

two loops	D / r	$\omega/2\kappa$	$Q = \omega/2\Gamma$	κ/Γ
r=1cm, a=1mm	3	82	1227	14.9
	5	379	1227	3.24
	7	1040	1227	1.18
	10	3033	1227	0.40
r=30cm,	3	175	1105	6.31
	5	810	1105	1.36
	7	2223	1105	0.50
	10	6481	1105	0.17
r=1m, a=4mm	3	193	1315	6.81
	5	891	1315	1.48
	7	2446	1315	0.54
	10	7131	1315	0.18

Figure 3: Analytical results for: (a) A loop of radius r of conducting wire, whose cross-section has radius a, loaded with a capacitor to enforce resonance at frequency $\omega = 1/\sqrt{LC}$. For the tabulated results one loop ($N=1$) of copper ($\rho = 1.69 \cdot 10^{-8} \Omega m$) wire was used, the dimensions were chosen to correspond to a few typical sizes of interest for applications, and the frequency of maximum Q was considered. (b) Medium-distance coupling between two such loops, achieved through the magnetic field produced into free space by their currents. The Γ's are taken to be the same as the corresponding single-cavity Γ's, namely interference effects have been neglected. [An example of dissimilar loops is that of $r=1m$ (source on the ceiling) loop and $r=30cm$ (household robot on the floor) loop at a distance $D=3m$ (room height) apart, for which $\kappa / \sqrt{\Gamma_1 \Gamma_2} = 0.88$ peaks at $f=6.4MHz$.]

III. Influence of extraneous objects

Clearly, the success of the proposed resonance-based wireless energy-transfer scheme depends strongly on the robustness of the objects' resonances. Therefore, their sensitivity to the near presence of random non-resonant extraneous objects is another aspect of the proposed scheme that requires analysis. The appropriate analytical model now is that of "perturbation theory" [6], which suggests that in the presence of an extraneous object e the field amplitude $a_1(t)$ inside the resonant object 1 satisfies, to first order:

$$\frac{da_1}{dt} = -i\left(\omega_1 - i\Gamma_1\right)a_1 + i\left(\kappa_{11-e} + i\Gamma_{1-e}\right)a_1 \tag{2}$$

where again ω_1 is the frequency and Γ_1 the intrinsic (absorption, radiation etc.) loss rate, while κ_{11-e} is the frequency shift induced onto 1 due to the presence of e and Γ_{1-e} is the extrinsic due to e (absorption inside e, scattering from e etc.) loss rate[**]. The frequency shift is a problem that can be "fixed" rather easily by applying to every device a feedback mechanism that corrects its frequency (e.g. through small changes in geometry) and matches it to that of the source. However, the extrinsic loss can be detrimental to the functionality of the energy-transfer scheme, because it cannot be remedied, so the total loss rate $\Gamma_{1[e]} = \Gamma_1 + \Gamma_{1-e}$ (and the corresponding figure-of-merit $\kappa_{[e]} / \sqrt{\Gamma_{1[e]}\Gamma_{2[e]}}$, where $\kappa_{[e]}$ the perturbed coupling rate) must be quantified[††].

a) Dielectric disks

In the first example of resonant objects that we have considered, namely dielectric disks, small, low-index, low-material-loss or far-away stray objects will induce small scattering and absorption. In such cases of small perturbations these extrinsic loss mechanisms can be quantified using respectively the analytic first-order formulas

[**] The first-order perturbation-theory model is really only valid for small perturbations. However, the parameters κ_{11-e}, Γ_{1-e} are still well defined, if a_1 is taken to be the amplitude of the exact perturbed mode.

[††] Note that interference effects between the radiation field of the initial resonant-object mode and the field scattered off the extraneous object can for strong scattering (e.g. off metallic objects) result in total radiation-Γ_{1e}'s that are smaller than the initial radiation-Γ_1 (namely Γ_{1-e} is negative!), as will be seen in the examples.

$\Gamma_{1-e}^{rad} \propto \omega_1 \cdot \int d^3\mathbf{r} \left|\mathrm{Re}\{\varepsilon_e(\mathbf{r})\}\right|^2 |\mathbf{E}_1(\mathbf{r})|^2 / U$ and $\Gamma_{1-e}^{abs} = \omega_1 / 4 \cdot \int d^3\mathbf{r}\, \mathrm{Im}\{\varepsilon_e(\mathbf{r})\} |\mathbf{E}_1(\mathbf{r})|^2 / U$, where $U = 1/2 \cdot \int d^3\mathbf{r} \varepsilon(\mathbf{r}) |\mathbf{E}_1(\mathbf{r})|^2$ is the total resonant electromagnetic energy of the unperturbed mode. As one can see, both of these losses depend on the *square* of the resonant electric field tails $\mathbf{E}_1$ at the site of the extraneous object. In contrast, the coupling rate from object 1 to another resonant object 2 is $\kappa_{21} = \omega_1 / 4 \cdot \int d^3\mathbf{r} \varepsilon_2(\mathbf{r}) \mathbf{E}_2^*(\mathbf{r}) \mathbf{E}_1(\mathbf{r}) / U$ and depends *linearly* on the field tails $\mathbf{E}_1$ of 1 inside 2. This difference in scaling gives us confidence that, for exponentially small field tails, coupling to other resonant objects should be much faster than all extrinsic loss rates ($\kappa \gg \Gamma_{1-e}$), at least for small perturbations, and thus the energy-trasnfer scheme is expected to be sturdy for this class of resonant dielectric disks.

However, we also want to examine certain possible situations where extraneous objects cause perturbations too strong to analyze using the above first-order perturbative approach. For example, we place a dielectric disk c close to another off-resonance object of large $\mathrm{Re}\{\varepsilon\}$, $\mathrm{Im}\{\varepsilon\}$ and of same size but different shape (such as a human being h), as shown in Figure 4a, and a roughened surface of large extent but of small $\mathrm{Re}\{\varepsilon\}$, $\mathrm{Im}\{\varepsilon\}$ (such as a wall w), as shown in Figure 4b. For distances $D_{h/w} / r = 10 - 3$ between the disk-center and the "human"-center/"wall", the numerical FDFD simulations presented in Figure 4 suggest that $Q_{c[h]}^{rad}, Q_{c[w]}^{rad} \geq 1000$ (instead of the initial $Q_c^{rad} \geq 2000$), $Q_c^{abs} \sim 10^4$ (naturally unchanged), $Q_{c-h}^{abs} \sim 5 \cdot 10^4 - 5 \cdot 10^2$, and $Q_{c-w}^{abs} \sim 10^5 - 10^4$, namely the disk resonance seems to be fairly robust, since it is not detrimentally disturbed by the presence of extraneous objects, with the exception of the *very* close proximity of high-loss objects.

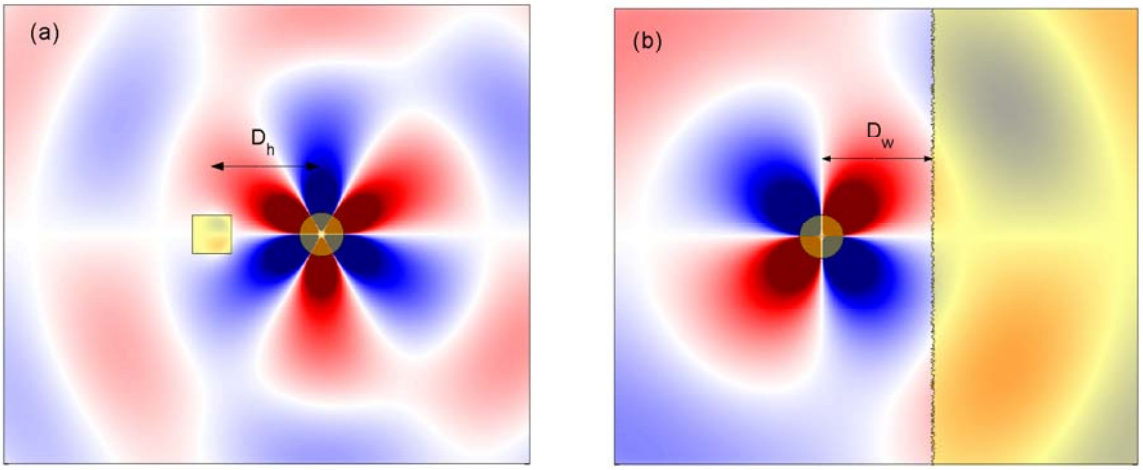

disk with "human"	D_h / r	$Q_{c[h]}^{rad}$	Q_{c-h}^{abs}	Q=ω/2Γ
Re{ε}=147.7, m=2	3	981	230	183
$\lambda / r \approx 20$	5	1984	2917	1057
$Q_c^{abs} \approx 10096$	7	2230	11573	1578
	10	2201	41496	1732
Re{ε}=65.6, m=3	3	6197	1827	1238
$\lambda / r \approx 10$	**5**	**11808**	**58431**	**4978**
$Q_c^{abs} \approx 10096$	7	9931	249748	4908
	10	9078	867552	4754

disk with "wall"	D_w / r	$Q_{c[w]}^{rad}$	Q_{c-w}^{abs}	Q=ω/2Γ
Re{ε}=147.7, m=2	3	1235	16725	1033
$\lambda / r \approx 20$	**5**	**1922**	**31659**	**1536**
$Q_c^{abs} \approx 10096$	7	2389	49440	1859
	10	2140	82839	1729
Re{ε}=65.6, m=3	3	6228	53154	3592
$\lambda / r \approx 10$	5	10988	127402	5053
$Q_c^{abs} \approx 10096$	7	10168	159192	4910
	10	9510	191506	4775

Figure 4: Numerical FDFD results for reduction in Q of a resonant disk due to scattering from and absorption in extraneous objects: (a) a high *ε=49+16i* (which is large but actually appropriate for human muscles in the GHz regime [13]) square object of same size (area) with the disk, and (b) a large roughened surface of *ε=2.5+0.05i* (appropriate for ordinary materials such as concrete, glass, plastic, wood [13]).For the tabulated results disk material loss Im{ε}/Re{ε}=10^{-4} was used and the mode that is odd with respect to the line that connects the two objects. An increase in radiation Q is again due to destructive interference effects. *{The specific parameters of the shown plots are highlighted with bold in the Tables.}*

To examine the influence of large perturbations on an entire energy-transfer system we consider two resonant disks in the close presence of both a "human" and a "wall". The numerical FDFD simulations show that the system performance deteriorates from κ / Γ_c (Figure 2) to $\kappa_{[hw]} / \Gamma_{c[hw]}$ (Figure 5) only by acceptably small amounts.

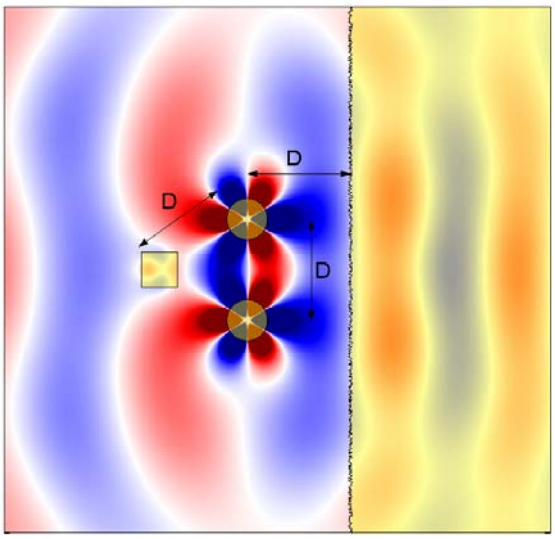

two disks with "human" and	D/r	$\omega/2\kappa$	$Q_{c[hw]}^{rad}$	Q_{c-h}^{abs}	Q_{c-w}^{abs}	$Q_c = \omega/2\Gamma_c$	κ/Γ_c
Re{ε}=147.7, m=2	3	48	536	3300	12774	426	8.8
$\lambda/r \approx 20$	5	322	1600	5719	26333	1068	3.3
$Q_c^{abs} \approx 10096$	7	973	3542	13248	50161	2097	2.2
	10	1768	3624	18447	68460	2254	1.3
Re{ε}=65.6, m=3	3	141	6764	2088	36661	1328	9.4
$\lambda/r \approx 10$	**5**	**2114**	**11945**	**72137**	**90289**	**4815**	**2.3**
$Q_c^{abs} \approx 10096$	7	8307	12261	237822	129094	5194	0.6

Figure 5: Numerical FDFD results for reduction in $\kappa/\sqrt{\Gamma_1\Gamma_2}$ of medium-distance coupling between two resonant disks due to scattering from and absorption in extraneous objects: both a high *ε=49+16i* square object of same size (area) with the disks and a large roughened surface of *ε=2.5+0.05i*. If initially all the energy is in one disk, after some time (*t=π/2κ*) both disks are equally excited to one of the normal modes of their combined system, while little energy has been lost due to the nearby extraneous objects. For the tabulated results the normal mode that is odd with respect to the line that connects the two disks is used, only distances for non-radiative ($D \le r_C$) coupling are considered, and the Γ's are taken to be the averages of the corresponding calculated Γ's of the two normal modes, where an increase/decrease in radiation Q for the system is due to destructive/constructive interference effects. *{The specific parameters of the shown plot are highlighted with bold in the Table.}*

b) Capacitively-loaded conducting-wire loops

In the second example of resonant objects that we have considered, the conducting-wire loops, the influence of extraneous objects on the resonances is nearly absent. The reason is that, in the quasi-static regime of operation (*r«λ*) that we are considering, the near field in the air region surrounding the loop is predominantly magnetic (since the electric field is localized inside

the capacitor), therefore extraneous objects e that could interact with this field and act as a perturbation to the resonance are those having significant magnetic properties (magnetic permeability *Re{μ}>1* or magnetic loss *Im{μ}>0*). Since almost all common materials are non-magnetic, they respond to magnetic fields in the same way as free space, and thus will not disturb the resonance of a conducting-wire loop, so we expect $\kappa_{[e]}/\Gamma_{[e]} \sim \kappa/\Gamma \sim 0.1-10$. The only perturbation that is expected to affect these resonances is a close proximity of large metallic structures. An extremely important implication of this fact relates to safety considerations for human beings. Humans are also non-magnetic and can sustain strong magnetic fields without undergoing any risk (a typical example where magnetic fields *B~1T* are safely used on humans is the Magnetic Resonance Imaging (MRI) technique for medical testing).

In comparison of the two classes of resonant systems under examination, the strong immunity to extraneous objects and the absence of risks for humans probably makes the conducting-wire loops the preferred choice for many real-world applications; on the other hand, systems of disks (or spheres) of high (effective) refractive index have the advantage that they are also applicable to much smaller length-scales (for example in the optical regime dielectrics prevail, since conductive materials are highly lossy).

IV. Efficiency of energy-transfer scheme

Consider again the combined system of a resonant source s and device d in the presence of a set of extraneous objects e, and let us now study the efficiency of this resonance-based energy-transfer scheme, when energy is being drained from the device at rate Γ_{work} for use into operational work. The coupled-mode-theory equation for the device field-amplitude is

$$\frac{da_d}{dt} = -i\left(\omega - i\Gamma_{d[e]}\right)a_d + i\kappa_{[e]}a_s - \Gamma_{work}a_d\,, \tag{3}$$

where $\Gamma_{d[e]} = \Gamma_{d[e]}^{rad} + \Gamma_{d[e]}^{abs} = \Gamma_{d[e]}^{rad} + \left(\Gamma_d^{abs} + \Gamma_{d-e}^{abs}\right)$ is the net perturbed-device loss rate, and similarly we define $\Gamma_{s[e]}$ for the perturbed-source. Different temporal schemes can be used to

extract power from the device (e.g. steady-state continuous-wave drainage, instantaneous drainage at periodic times and so on) and their efficiencies exhibit different dependence on the combined system parameters. Here, we assume steady state, such that the field amplitude inside the source is maintained constant, namely $a_s(t) = A_s e^{-i\omega t}$, so then the field amplitude inside the device is $a_d(t) = A_d e^{-i\omega t}$ with $A_d / A_s = i\kappa_{[e]} / (\Gamma_{d[e]} + \Gamma_{work})$. Then, the useful extracted power is $P_{work} = 2\Gamma_{work} |A_d|^2$, the radiated (including scattered) power is $P_{rad} = 2\Gamma_{s[e]}^{rad} |A_s|^2 + 2\Gamma_{d[e]}^{rad} |A_d|^2$, the power absorbed at the source/device is $P_{s/d} = 2\Gamma_{s/d}^{abs} |A_{s/d}|^2$, and at the extraneous objects $P_e = 2\Gamma_{s-e}^{abs} |A_s|^2 + 2\Gamma_{d-e}^{abs} |A_d|^2$. From energy conservation, the total power entering the system is $P_{total} = P_{work} + P_{rad} + P_s + P_d + P_e$. Depending on the targeted application, reasonable choices for the work-drainage rate are: $\Gamma_{work} = \Gamma_{d[e]}$ (the common impedance-matching condition) to minimize the required energy stored in the source or $\Gamma_{work} = \Gamma_{d[e]} \cdot \sqrt{1 + fom_{[e]}^2} > \Gamma_{d[e]}$ to maximize the working efficiency $\eta_{work} = P_{work} / P_{total}$ for some value of the distance-dependent figure-of-merit $fom_{[e]} = \kappa_{[e]} / \sqrt{\Gamma_{s[e]} \Gamma_{d[e]}}$ of the perturbed resonant energy-exchange system. For both choices, η_{work} is a function of this parameter only. It is shown for the optimal choice in Figure 6 with a solid black line, and is $\eta_{work} > 15\%$ for $fom_{[e]} > 1$, namely large enough for practical applications. The loss conversion ratios depend also on the other system parameters, and the most disturbing ones (radiation and absorption in stray objects) are plotted in Figure 6 for the two example systems of dielectric disks and conducting loops with values for their parameters within the ranges determined earlier.

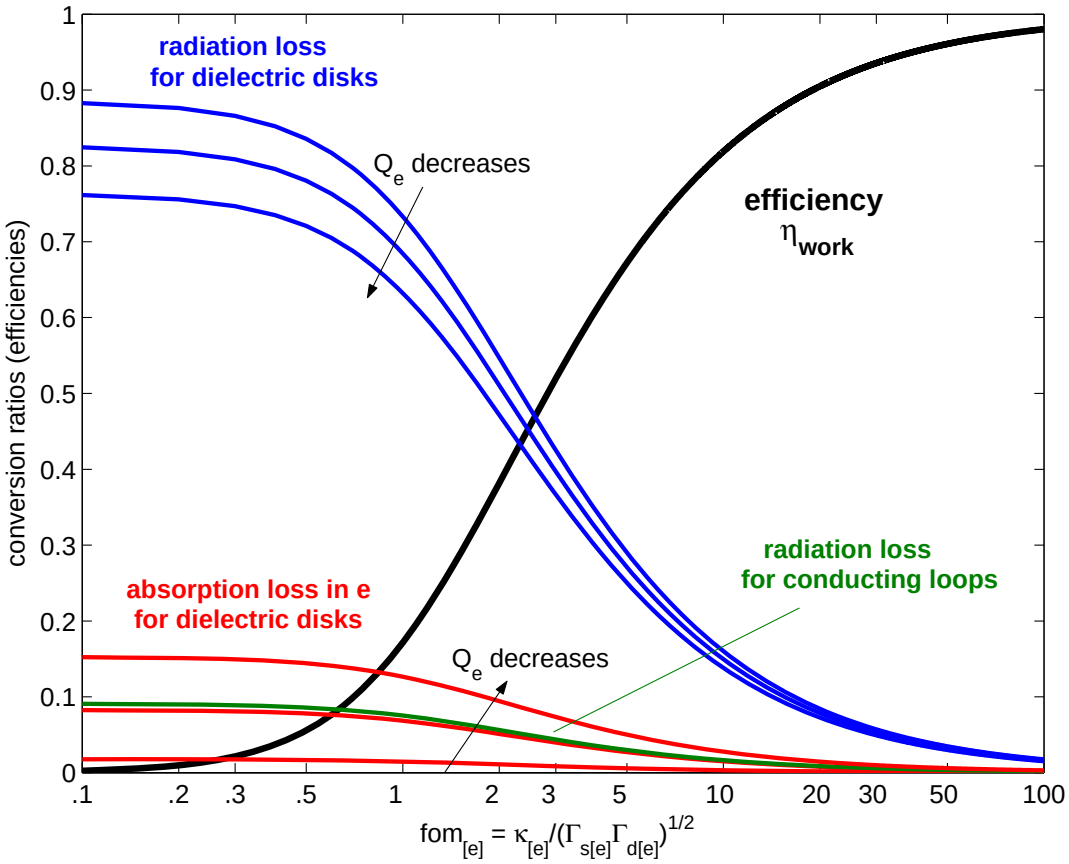

Figure 6: (Black line) Efficiency of converting the supplied power into useful work (η_{work}) as a function of the perturbed coupling-to-loss figure-of-merit, optimized with respect to the power-extracting rate Γ_{work} (related to the load impedance), for all values of the various quality factors that are present in the system. (Blue and red lines) Ratios of power conversion respectively into radiation (including scattering from nearby extraneous objects) and dissipation inside an extraneous object as a function of the figure-of-merit for dielectric disks of $Q_{s[e]}^{rad} = Q_{d[e]}^{rad} \sim 10^3$ and $Q_s^{abs} = Q_d^{abs} \sim 10^4$, and for three values of $Q_{s-e}^{abs} = Q_{d-e}^{abs} = 10^4,\ 5\cdot 10^4,\ 10^5$. (Green line) Ratio of power conversion into radiation for conducting-wire loops of $Q_{s[e]}^{rad} = Q_{d[e]}^{rad} \sim 10^4$ and $Q_s^{abs} = Q_d^{abs} \sim 10^3$, and assuming $Q_{s-e}^{abs} = Q_{d-e}^{abs} \to \infty$.

To get a numerical estimate for a system performance, take, for example, coupling distance $D/r = 5$, a "human" extraneous object at distance $D_h/r = 10$, and that $P_{work} = 10W$ must be delivered to the load. Then, for dielectric disks we have $Q_{s[h]}^{rad} = Q_{d[h]}^{rad} \sim 10^3$, $Q_s^{abs} = Q_d^{abs} \sim 10^4$, $Q_{s-h}^{abs} = Q_{d-h}^{abs} \sim 5\cdot 10^4$ and $fom_{[h]} \sim 5$, so from Figure 6 we find that $P_{rad} \approx 4.4W$ will be radiated to free space, $P_s \approx 0.3W$ will be dissipated inside the source, $P_d \approx 0.2W$ inside the device, and $P_h \approx 0.1W$ inside the human. On the other hand, for conducting loops we have $Q_{s[h]}^{rad} = Q_{d[h]}^{rad} \sim 10^4$, $Q_s^{abs} = Q_d^{abs} \sim 10^3$, $Q_{s-h}^{abs} = Q_{d-h}^{abs} \to \infty$ and $fom_{[h]} \sim 2$, so we find $P_{rad} \approx 1.5W$, $P_s \approx 11W$, $P_d \approx 4W$, and most importantly $P_h \to 0$.

V. Conclusion

In conclusion, we present a resonance-based scheme for mid-range wireless non-radiative energy transfer. Although our consideration has been for a static geometry (namely κ and Γ_e were independent of time), all the results can be applied directly for the dynamic geometries of mobile objects, since the energy-transfer time κ^{-1} ($\sim 1-100\mu s$ for microwave applications) is much shorter than any timescale associated with motions of macroscopic objects. Analyses of very simple implementation geometries provide encouraging performance characteristics and further improvement is expected with serious design optimization. Thus the proposed mechanism is promising for many modern applications. For example, in the macroscopic world, this scheme could be used to deliver power to robots and/or computers in a factory room, or electric buses on a highway (source-cavity would in this case be a "pipe" running above the highway). In the microscopic world, where much smaller wavelengths would be used and smaller powers are needed, one could use it to implement optical inter-connects for CMOS electronics, or to transfer energy to autonomous nano-objects (e.g. MEMS or nano-robots) without worrying much about the relative alignment between the sources and the devices.

As a venue of future scientific research, enhanced performance should be pursued for electromagnetic systems either by exploring different materials, such as plasmonic or metallodielectric structures of large effective refractive index, or by fine-tuning the system design, for example by exploiting the earlier mentioned interference effects between the radiation fields of the coupled objects. Furthermore, the range of applicability could be extended to acoustic systems, where the source and device are connected via a common condensed-matter object.

ACKNOWLEDGEMENTS

We deeply thank Prof. John Pendry and L. J. Radziemski for suggesting magnetic and acoustic resonances respectively, Prof. Steven G. Johnson and André Kurs for the useful discussions, and to Miloš Popović for providing his FDFD mode-solver. This work was supported in part by the Materials Research Science and Engineering Center program of the National Science Foundation under Grant No. DMR 02-13282.

REFERENCES

1) Tesla, N. Apparatus for transmitting electrical energy. *U.S. patent* number 1,119,732, issued in December 1914.

2) Esser, A. and Skudelny, H.-C. A new approach to power supplies for robots. *IEEE Trans. on industry applications* **27**, 872 (1991).

3) Hirai, J., Kim, T.-W. and Kawamura, A. Wireless transmission of power and information and information for cableless linear motor drive. *IEEE Trans. on power electronics* **15**, 21 (2000).

4) Fernandez, J. M. and Borras, J. A. Contactless battery charger with wireless control link. *U.S. patent* number 6,184,651, issued in February 2001.

5) SplashPower Ltd. (www.splashpower.com).

6) Haus, H. A. *Waves and Fields in Optoelectronics* (Prentice-Hall, New Jersey, 1984).

7) Pozar, D. M. *Microwave Engineering* (Wiley, New Jersey, 2005).

8) Jacob, M. V. Lithium Tantalate - A High Permittivity Dielectric Material for Microwave Communication Systems. *Proc. of IEEE TENCON 2003* **4**, 1362 (2003).

9) Raether, H. *Surface Plasmons* (Springer-Verlag, Berlin, 1988).

10) Sievenpiper, D. F. *et al.* 3D Metallo-Dielectric Photonic Crystals with Strong Capacitive Coupling between Metallic Islands. *Phys. Rev. Lett.* **80**, 2829 (1998).

11) Grover, F. *Inductance Calculations: Working Formulas and Tables*, (Dover Publications Inc., New York, 1946).

12) Balanis, C. A. *Antenna Theory: Analysis and Design* (Wiley, New Jersey, 2005).

13) Fenske, K. and Misra, D. K. Dielectric materials at microwave frequencies. *Applied Microwave and Wireless* **12**, 92 (2000).